Cross-Country Faults in Resonant-Grounded Networks: Mathematical Modelling, Simulations and Field Recordings

G.M.G. Guerreiro, Z. Gajić, S. Zubić, N. Taylor, Md Z. Habib

***Abstract*—Cross-Country Faults (CCFs) are defined by the occurrence of two Single Phase-to-Ground faults taking place simultaneously in different phases and at different locations of the galvanically connected network. Few studies about these faults in MV systems have been done so far, particularly with real fault data and simulations. In this work, first a mathematical model is derived to understand basic properties of CCFs. Then, simulations in RSCAD/RTDS® using real data obtained from an utility in Scandinavia are discussed and validated with two real faults measured in the field for Resonant-Grounded networks in Sweden and Norway. The mathematical calculations proved to have a good accuracy and showed important properties of CCFs such as the dependency of both faults of each others fault resistance and location. Furthermore, it was observed that such faults can be very different from more common types of faults in the Power System. Interesting behaviors can appear particularly when feeders are connected in ring, where an extra current with smaller magnitude and 180° appears on the measurement point, as well as in lines with double infeed where a very large difference is detected depending on the fault location which influences directly both ends of the line.**

***Keywords*—Cross-country fault; resonant grounding; compensated network; MV network; fault analysis; RSCAD/RTDS.**

I. Introduction

RELIABILITY requirements for power systems have been constantly increasing, as customers of electric power desire high power availability. In order to improve continuity of supply in medium voltage (MV) networks, many utilities around the world use resonant grounding. In such systems, customers are commonly connected through Dy transformers and phase-to-phase voltages are not disturbed during a single phase-to-ground fault. Therefore, some of the utilities allow continuation of supply for periods from several seconds up to several hours, since the ground-fault current at the fault point in such systems is considerably reduced and is unlikely to damage equipment or create hazardous voltages for people or livestock [1],[2],[3].

Due to the neutral potential displacement during a phase-to-ground fault, the healthy phase voltages can rise to 1.73 times the nominal values in the entire network, over-stressing insulation and increasing the probability of a second phase-to-ground fault somewhere else in the network. The situation of two simultaneously active phase-to-ground faults on different phases at different locations in a network is commonly called a Cross-Country fault (CCF) or Double-Ground fault [4],[5],[6]. During these faults, the currents flowing through the phases and, importantly, ground becomes many times higher than in the case of a single phase-to-ground in such systems, thus necessitating fast and selective operation of relay protection [1].

In the event of a CCF, some utilities opt to identify the two faulted phases and only trip one of the two faults returning to a state where only one single phase-to-ground fault exists. The power system is then allowed to operate and continues to supply power to the loads. This scheme is commonly identified as Phase-Preference Logic or Double-Ground Preference Logic [4],[7]. Thus understanding how these CCFs can be calculated and the behavior of currents and voltages that can appear in the system are crucial for correct protection operation in resonant-grounded systems.

Considering the above, this paper aims to derive a simple mathematical model for CCFs as well as to explore the current and voltage patterns that these faults can present in resonant-grounded systems. Simulation of various CCFs is done in RSCAD® and validation of these results was done by actual recordings obtained from utilities in Scandinavia.

II. Mathematical Modelling

Mathematical models are often very valuable to provide a more clear understanding on how faults behave. In the case of CCFs, this modelling has been rarely explained and expanded upon before. Consider Fig. 1 showing a simple single-line diagram of two radial three-phase feeders connected to a common bus.

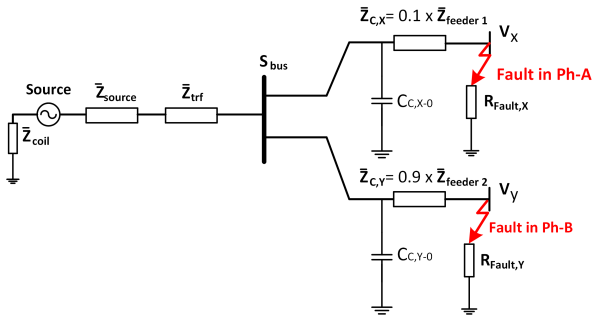

Fig. 1. System for mathematical model.

G. M. G. Guerreiro, S. Zubić and Z. Gajić are with Hitachi ABB Power Grids, Nätverksgatan 3, 721 36 Västerås, Sweden (e-mail of corresponding author: gabriel.guerreiro@hitachi-powergrids.com).

N. Taylor and Md Z. Habib are with KTH Royal Institute of Technology, Teknikrigen 31, 114 28 Stockholm, Sweden.

Paper submitted to the International Conference on Power Systems Transients (IPST2021) in Belo Horizonte, Brazil June 06-10, 2021.

A Petersen coil impedance $\overline{Z}_{\text{coil}}$ is connected in the neutral point and for simplicity, the total three-phase shunt capacitance to ground of each cable is connected at the beginning of the cable. Two single-phase-to-ground faults (SPGF) are applied simultaneously, in Phase A at $10\ \%$ of the first feeder (Fault Location X) and in Phase B at $90\ \%$ of the other feeder (Fault Location Y), where each fault has its own fault resistance represented by $R_{\text{fault,X}}$ and $R_{\text{fault,Y}}$, respectively.

The system above can be represented in Fig. 2 by three Two-Port networks using Z (impedance) parameters, connected in series since two SPGFs are occurring. This type of representation is commonly used to represent many types of simultaneous faults and it is further described in [8]-[9].

Since the first fault is in Phase A in location X and in phase with the internal positive sequence voltage source $\overline{U}_{\text{X,i}}$, there is no need to include phase shifting transformers in the model. However, for the second fault in Phase B located in Y, it is necessary to phase shift the positive and negative sequence components before connecting them in series across the fault resistance.

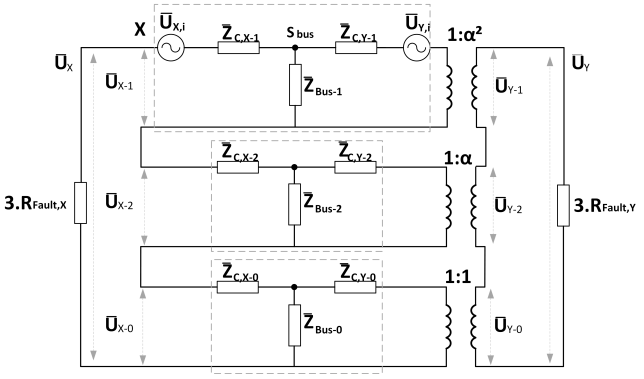

Fig. 2. Symmetrical component representation of two-port connected in series.

The internal positive sequence voltage sources $\overline{U}_{\text{X,i}}$ and $\overline{U}_{\text{Y,i}}$ can be considered as having the nominal phase-to-ground magnitude for short-circuit calculations and $\overline{Z}_{\text{bus-}x}$ can be defined as:

$$\overline{Z}_{\text{bus-1}} = \overline{Z}_{\text{bus-2}} = \overline{Z}_{\text{source}}$$

$$\overline{Z}_{\text{bus-0}} = \overline{Z}_{\text{coil}} // \frac{1}{j\omega(C_{\text{C,X-0}} + C_{\text{C,Y-0}})}$$

Based on Fig. 2 and theory presented in [6], [8] and [9], it is possible to write down the two-port equations for positive, negative and zero sequence components as in (1), (2) and (3) respectively.

$$\begin{bmatrix}\overline{U}_{\text{X-1}}\\ \overline{U}_{\text{Y-1}}\end{bmatrix} = \begin{bmatrix}1\cdot\overline{U}_{\text{X,i}}\\ \alpha^2\cdot\overline{U}_{\text{Y,i}}\end{bmatrix} - \begin{bmatrix}\overline{Z}_{\text{C,X-1}} & \alpha\cdot\overline{Z}_{\text{bus-1}}\\ \alpha^2\cdot\overline{Z}_{\text{bus-1}} & \overline{Z}_{\text{C,Y-1}}\end{bmatrix}\cdot\begin{bmatrix}\overline{I}_{\text{X-1}}\\ \overline{I}_{\text{Y-1}}\end{bmatrix} \quad (1)$$

$$\begin{bmatrix}\overline{U}_{\text{X-2}}\\ \overline{U}_{\text{Y-2}}\end{bmatrix} = -\begin{bmatrix}\overline{Z}_{\text{C,X-2}} & \alpha^2\cdot\overline{Z}_{\text{bus-2}}\\ \alpha\cdot\overline{Z}_{\text{bus-2}} & \overline{Z}_{\text{C,Y-2}}\end{bmatrix}\cdot\begin{bmatrix}\overline{I}_{\text{X-2}}\\ \overline{I}_{\text{Y-2}}\end{bmatrix} \quad (2)$$

$$\begin{bmatrix}\overline{U}_{\text{X-0}}\\ \overline{U}_{\text{Y-0}}\end{bmatrix} = -\begin{bmatrix}\overline{Z}_{\text{C,X-0}} & \overline{Z}_{\text{bus-0}}\\ \overline{Z}_{\text{bus-0}} & \overline{Z}_{\text{C,Y-0}}\end{bmatrix}\cdot\begin{bmatrix}\overline{I}_{\text{X-0}}\\ \overline{I}_{\text{Y-0}}\end{bmatrix} \quad (3)$$

The sequence voltages can be equated to the voltage across the fault resistance on the secondary of the phase shifting transformer as in (4). If the fault in any of the two fault locations is solid (fault resistance is $0\ \Omega$), the sum of sequence voltages will be equal to approximately 0 V. Furthermore, the sequence current components on each side with a single phase-to-ground fault have all the same value as well and can be equated for simplification as shown in (5).

$$\begin{bmatrix}\overline{U}_{\text{X}}\\ \overline{U}_{\text{Y}}\end{bmatrix} = \begin{bmatrix}\overline{U}_{\text{X-1}}\\ \overline{U}_{\text{Y-1}}\end{bmatrix} + \begin{bmatrix}\overline{U}_{\text{X-2}}\\ \overline{U}_{\text{Y-2}}\end{bmatrix} + \begin{bmatrix}\overline{U}_{\text{X-0}}\\ \overline{U}_{\text{Y-0}}\end{bmatrix} = \begin{bmatrix}3\cdot R_{\text{fault,X}} & 0\\ 0 & 3\cdot R_{\text{fault,Y}}\end{bmatrix}\cdot\begin{bmatrix}\overline{I}_{\text{X,seq}}\\ \overline{I}_{\text{Y,seq}}\end{bmatrix} \quad (4)$$

$$\begin{bmatrix}\overline{I}_{\text{X,seq}}\\ \overline{I}_{\text{Y,seq}}\end{bmatrix} = \begin{bmatrix}\overline{I}_{\text{X-1}}\\ \overline{I}_{\text{Y-1}}\end{bmatrix} = \begin{bmatrix}\overline{I}_{\text{X-2}}\\ \overline{I}_{\text{Y-2}}\end{bmatrix} = \begin{bmatrix}\overline{I}_{\text{X-0}}\\ \overline{I}_{\text{Y-0}}\end{bmatrix} \quad (5)$$

Substituting (1),(2), (3) and (5) into (4), it is possible to obtain (6), where the currents in both locations are calculated.

$$\begin{bmatrix}\overline{I}_{\text{X,seq}}\\ \overline{I}_{\text{Y,seq}}\end{bmatrix} = \begin{bmatrix}\overline{Z}_{\text{X,X}} & \overline{Z}_{\text{X,Y}}\\ \overline{Z}_{\text{Y,X}} & \overline{Z}_{\text{Y,Y}}\end{bmatrix}^{-1}\cdot\begin{bmatrix}1\cdot\overline{U}_{\text{X,i}}\\ \alpha^2\cdot\overline{U}_{\text{Y,i}}\end{bmatrix} \quad (6)$$

where,

- $\overline{Z}_{\text{X,X}} = \overline{Z}_{\text{C,X-1}} + \overline{Z}_{\text{C,X-2}} + \overline{Z}_{\text{C,X-0}} + 3\cdot R_{\text{fault,X}}$
- $\overline{Z}_{\text{Y,Y}} = \overline{Z}_{\text{C,Y-1}} + \overline{Z}_{\text{C,Y-2}} + \overline{Z}_{\text{C,Y-0}} + 3\cdot R_{\text{fault,Y}}$
- $\overline{Z}_{\text{X,Y}} = \alpha\cdot\overline{Z}_{\text{bus-1}} + \alpha^2\cdot\overline{Z}_{\text{bus-2}} + \overline{Z}_{\text{bus-0}}$
- $\overline{Z}_{\text{Y,X}} = \alpha^2\cdot\overline{Z}_{\text{bus-1}} + \alpha\cdot\overline{Z}_{\text{bus-2}} + \overline{Z}_{\text{bus-0}}$

The voltages and currents at both fault locations can then be also calculated based on previously shown (4) and (6). Fault Location Y is described below as an example in (7) and (8), where the phase-shifting due to transformers in the model is also taken into account. The magnitudes in location X can also be easily calculated, for which phase-shifting transformers are not needed since the faulted Ph-A is in phase with the internal positive sequence voltage sources.

$$\begin{bmatrix}\overline{U}_{\text{Y,AN}}\\ \overline{U}_{\text{Y,BN}}\\ \overline{U}_{\text{Y,CN}}\end{bmatrix} = \begin{bmatrix}1 & 1 & 1\\ 1 & \alpha^2 & \alpha\\ 1 & \alpha & \alpha^2\end{bmatrix}\cdot\begin{bmatrix}\overline{U}_{\text{Y-0}}\\ \overline{U}_{\text{Y-1}}\\ \overline{U}_{\text{Y-2}}\end{bmatrix}\cdot\begin{bmatrix}1\\ \alpha\\ \alpha^2\end{bmatrix} \quad (7)$$

$$\begin{bmatrix}\overline{I}_{\text{Y,A}}\\ \overline{I}_{\text{Y,B}}\\ \overline{I}_{\text{Y,C}}\end{bmatrix} = \begin{bmatrix}1 & 1 & 1\\ 1 & \alpha^2 & \alpha\\ 1 & \alpha & \alpha^2\end{bmatrix}\cdot\overline{I}_{\text{Y}}\cdot\begin{bmatrix}1\\ \alpha\\ \alpha^2\end{bmatrix} \approx \begin{bmatrix}0\\ \overline{I}_{\text{Y,B}}\\ 0\end{bmatrix} \quad (8)$$

Using the information in the fault location, it is possible to calculate the voltage at any point of the network by summing up the voltage drop across the equivalent sequence impedances between the fault point and the desired bus. The calculation can be performed from either fault point to the bus.

Based on the demonstration and results shown above, the conclusions from the mathematical modelling can be summed up in three main points:

- The fault resistance in each fault location influences both faulted currents, since these currents enclose the same path through the fault resistance. This effect can be naturally deduced from reflecting on the CCF loop and also can be seen observed mathematically due to the inversion of the impedance matrix in (6).
- The currents at each fault location depend on the pre-fault positive sequence voltage value at each fault location as well as the relative distance between two faults.

- For very complex networks, an approach using the equivalent impedance matrix with mutual and diagonal impedances derived from the network's admittance matrix is recommended. This approach is further explored in [8]-[9]. By the end, the entire network is summed up again as a two-port network and the remaining process demonstrated previously is valid.

Finally, the network presented in the previous section was also simulated in the EMTP program RSCAD® and the simulation and results were compared. Table I shows the comparison for the case where both faults have 5 Ω resistance.

TABLE I
COMPARISON OF RESULTS FOR 5 Ω FAULT RESISTANCE AT EACH FAULT LOCATION.

Variable	Calculated	Simulated	Unit
$\overline{I}_{X,A}$	$2.34\angle -14.93°$	$2.34\angle -15.8°$	kA
$\overline{I}_{Y,B}$	$2.34\angle 165.53°$	$2.30\angle 164.2°$	kA
$\overline{U}_{X,AN}$	$11.72\angle -14.93°$	$11.69\angle -15.4°$	kV
$\overline{U}_{X,BN}$	$32.78\angle -145.2°$	$32.23\angle -145.5°$	
$\overline{U}_{X,CN}$	$37.72\angle 137.55°$	$37.76\angle 136.79°$	
$\overline{U}_{Y,AN}$	$20.30\angle 22.17°$	$20.57\angle 22.6°$	kV
$\overline{U}_{Y,BN}$	$11.71\angle 165.15°$	$11.708\angle 165°$	
$\overline{U}_{Y,CN}$	$41.09\angle 121.69°$	$41.26\angle 121.2°$	
$\overline{U}_{Sbus,AN}$	$13.03\angle -3.16°$	$13.276\angle -2.1°$	kV
$\overline{U}_{Sbus,BN}$	$31.73\angle -145.93°$	$31.32\angle -146°$	
$\overline{U}_{Sbus,CN}$	$37.9\angle 135.8°$	$37.82\angle 135.3°$	

III. CCF SIMULATIONS AND COMPARISON WITH REAL FAULTS

The overall single-line diagram of the simulated power system topology is given in Fig. 3. It was adapted from a real meshed 50 Hz, 47 kV MV network based on real data obtained from a Norwegian utility. The system is fed from three different sources with decentralized compensation (Petersen Coils connected in all three neutral points) and downstream loads are connected through Dy transformers.

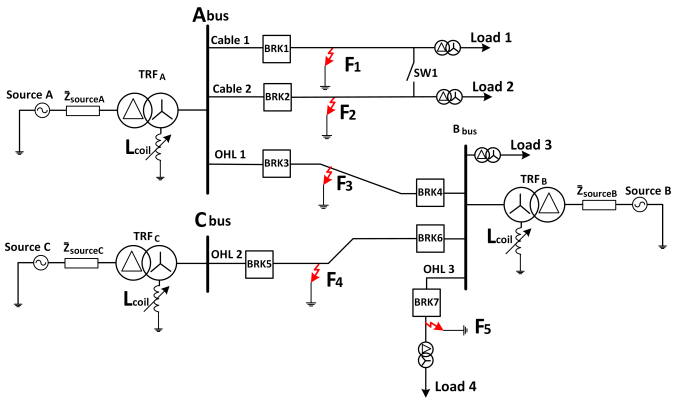

Fig. 3. Overall single-line diagram for the simulated system.

Some relevant considerations about the simulations are:

- During pre-fault conditions, the simulated system model is completely balanced.
- The libraries within RSCAD for all components in the figure were used. The Bergeron model was used for simulating all cables and lines.
- All faults applied had fixed resistance, i.e not arcs.
- A large number (in the range of thousands) of simulations were performed in order to identify and validate the described patterns.

Table II below shows the parameters of the simulated system.

TABLE II
SYSTEM'S PARAMETERS.

Variable	Value
Nominal Ph-Ph Voltage at MV system	47 kV
Nominal Ph-E Voltage at MV system	27.135 kV
TRF 1 Rated Power	300 MVA
TRFs 2 and 3 Rated Power	155 MVA
TRFs 1, 2 and 3 Primary Rated Voltage	420 kV
TRFs % Impedance	15 %
Total System's Capacitance	36 μF
Petersen Coils rated current	120 A
Petersen Coils inductance	0.7 H
Parallel Neutral Resistors	3000 Ω
Loads 1 and 2	20 MVA
Loads 3 and 4	10 MVA
Length of OHL1 and OHL2	20 km
Length of OHL3	15 km
Pos. Seq. Series Impedance of the OHLs	$0.07631 + j0.37763$ Ω/km
Zero Seq. Series Impedance of the OHLs	$0.2171 + j1.5802$ Ω/km
Length of Cables 1 and 2	20 km
Pos. Seq. Series Impedance of the Cables	$0.143 + j0.34$ Ω/km
Zero Seq. Series Impedance of the Cables	$0.382 + j1.021$ Ω/km

Two main fault combinations are explored in this paper. The first combination is between faults F1 and F2, which explores characteristics of CCFs in radial and ring connected feeders with single infeed, described as Types I and II. The second combination is between faults F1 and F3, which explores the characteristics of lines with double infeed, described as Types III and IV. Other faults types and combinations involving F4 and F5 were also simulated for confirmation of results, but are not presented here.

In the following subsections, the four different types of Cross-Country Faults and associated voltage and current patterns will be explored and explained. These patterns (from Type 1 to Type 4) can provide an useful resource for future research to use as benchmark for simulations and evaluation of specific power systems. The simulations are compared with real CCF recordings.

For a quick summary, the following four patterns are discussed and further explained here:

- **Type I**: Feeder with single infeed connected radially;
- **Type II**: Feeder with single infeed connected in ring;
- **Type III**: Line with double infeed where protection relay is located between the two faults;
- **Type IV**: Line with double infeed with the two faulted points located in front of protection relay;

A. Type I - Feeders with Single Infeed connected Radially

Many MV networks have the structure of multiple feeders connected in radial or ring manner with a single infeed connection from the main bus where the step-down transformer is connected. Figure 4 shows a simplified version

of the overall system of Fig. 3 with an equivalent source connected to A_{bus} representing the entire system connected behind it.

The following scenario is considered for evaluation where the first fault combination is used, between fault locations F1 and F2, where SW1 is open connecting both feeders (Cables 1 and 2) radially. The Cross-Country fault is simulated between Phases A (red, F1) and C (blue, F2), where a single phase-to-ground fault is already ongoing in Phase C in Cable 2 and at roughly 0.56 seconds another ground fault occurs in Cable 1 in Phase A.

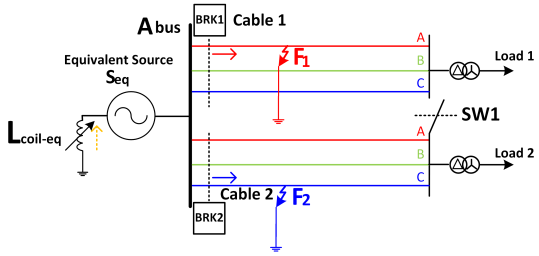

Fig. 4. Three-Phase representation of fault between points F1 and F2.

Recording obtained on the Norwegian network for a real CCF is compared below with the simulated results. The phase-to-ground voltages in the three phases are shown in Fig. 5, where the simulations were validated and show very similar results. It can be observed that during the first ground fault, the two healthy phase voltages have roughly nominal phase-to-phase voltage (47 kV) and at 0.56 seconds the second ground fault happens in the other feeder.

In this case, for the simulated signal the fault in Phase C (blue) at 10 % of Cable 2 is closer to the measurement point and the voltage magnitude is quite small while the fault in Phase A (red) at 70 % of Cable 1 is far away and therefore the voltage builds up from the faulty point up to the measurement point at the bus. It can be also seen that the voltage in the healthy phase is greater than both of the faulted phases, which can be further used to perform a type of phase selection.

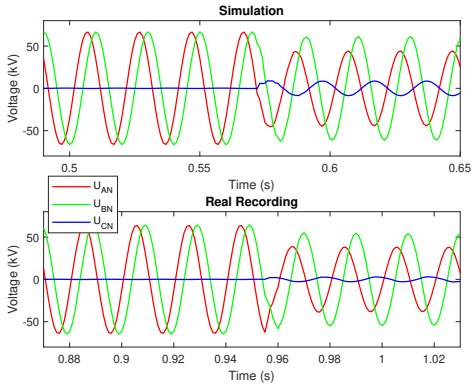

Fig. 5. Comparison of voltages between simulation and real recording for radial feeder [1].

The current's behavior is shown in Fig. 6, where the simulation and real recording are again compared. This pattern of CCF is one of the simplest for protection relays to handle. In this case, a slight difference in magnitude and DC component can be identified along with slight out of phase measurements. This difference in the phases can be mainly explained by the slightly different line zero-sequence impedance parameters of real network and one used in the simulation.

However, the main feature of such a fault in a purely radial feeder is that high current magnitude is only measured in one of the two faulted phases and thus the fault appears very similar to a single phase-to-ground fault in a solidly grounded system. The same current then returns through another phase in the second faulty feeder, which also shows familiar patterns of a SPGF.

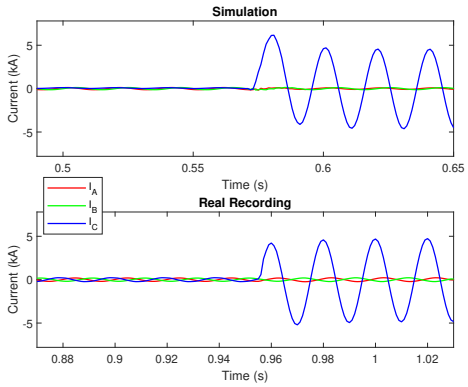

Fig. 6. Comparison of currents between simulation and real recording for radial feeder [1].

B. Type II - Feeders with Single Infeed connected in Ring

The situation studied in this Subsection is again based on Fig. 4, where faults are performed with switch SW1 closed to make the two cables part of a ring. However, in this case fault F2 in Phase C is at 50 % of Cable 2, and fault F1 in Phase A is at 80 % of Cable 1. This change was made in order to observe other effects in CCFs, especially in current magnitudes since faults need to be closer to each other to observe a reasonable current in the second faulty phase.

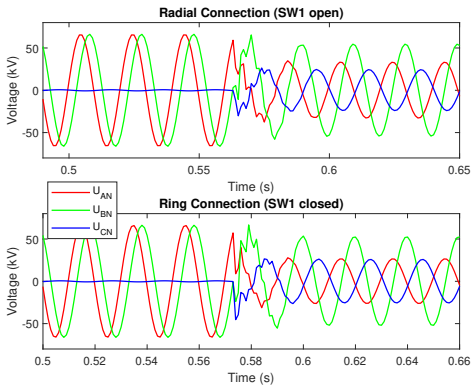

Fig. 7. Voltages at BRK2 for simulated faults comparing radial and ring connections.

Analyzing the voltages in Fig. 7 measured in the bus it is seen that the behavior between radial and ring connections is very similar apart from the fact that the voltages in ring have roughly the same magnitude due to the closing of SW1 and extra current flowing at each feeder.

The considerable effect of having feeders connected in ring can be observed in the current signals in Fig. 8 and also in the comparison performed in Fig.9 which shows residual current and faulted phase outside (Ph-A) the zone in % of the faulted phase inside the zone (Ph-C). An additional phase current $180°$ shifted flows also through the feeder Cable 1, feeding the fault in the other feeder cable through the ring connection.

Figure 9 shows that when fault F1 (supervised by the relay at BRK1) in the neighboring feeder moves from A_{bus} (shown in Fig. 4) to the end of the ringed feeder, it consequently becomes closer to the relay at BRK2 and therefore the current contribution in Phase A flowing through BRK2 increases. Since the currents in the two faulted phases are shifted $180°$, the measured residual current consequently decreases.

Thus, when fault F1 is at 0% of the Cable 1, the measured residual current I_N at feeder 2 is roughly 100% of faulted phase current I_C since fault F1 from BRK2's perspective is very far away. This behavior is really similar to a single phase-to-ground fault in a solid grounded system ($I_C = I_N$). However, when fault F1 is moved to the end of the feeder, almost the same distance from BRK1 and BRK2, the measured residual current is roughly 35% of the faulted phase current magnitude.

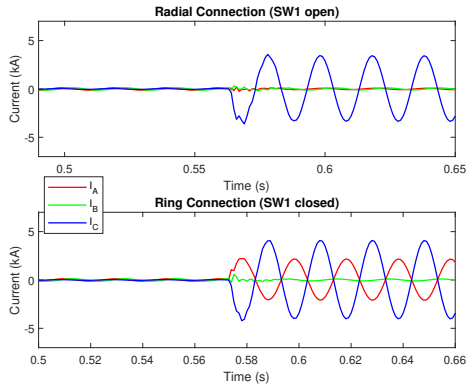

Fig. 8. Currents at BRK2 for simulated faults comparing radial and ring connections.

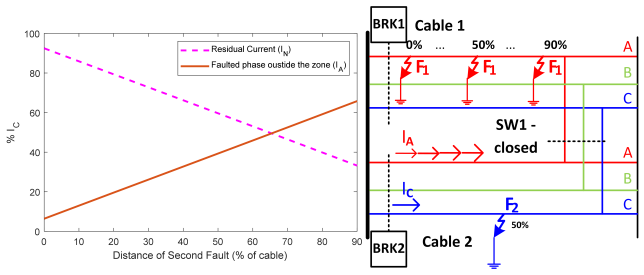

Fig. 9. Effects on currents in BRK2 from variation of distance of fault F1 (oustide the zone) from the A_{bus}.

The consequences of this effect can be specially problematic for impedance based or residual current based protections, which rely on high values of residual current in order to operate correctly.

C. Types III and IV - Line with Double Infeed

Fault combination 2, combining fault locations F1 and F3, is used in this case to define the two remaining CCF Type III and Type IV. Since Cross-Country faults often occur in different lines, Types III and IV will in most cases be present together in the protected network during a CCF fault. However, it might be possible that the CCF occurs in two different phases and two different locations but on the same line. In that case, both sides of the line would have a similar behaviour as BRK4 as discussed further.

An example of the distribution of currents from two sources can be seen in Fig. 10 where fault location F1 has a fault in Phase C and fault location F3 has faulted Phase A.

Figure 10 shows that the current flowing from one faulted point will almost entirely return through the other phase, passing through the ground path. A small part of the current (residual current) which does not return through the other faulted phase is referred to the summation, in the fault location, of the inductive currents (originated from the Petersen coils) and the capacitive current (from the total ground capacitances of the network). This residual current is highly dependent on the characteristics of the system compensation (over or undercompensated) and also the distribution of zero sequence voltages across the system during a CCF.

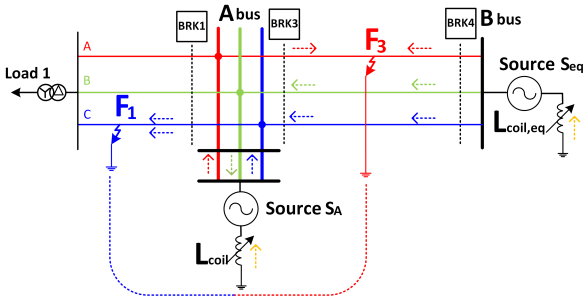

Fig. 10. Three-Phase representation of fault between points F1 and F3.

The Type IV current and voltage patterns can be seen in Fig. 11. In this case, BRK4 sees mainly a variant of a phase-to-phase fault which is connected through ground but does not have a significant return path through the neutral point of the transformers since the system is grounded via Petersen coils. Thus, almost the entire current flowing through one fault location will return through the other faulted point.

The only residual current actually flowing through BRK4 is originated from the Petersen coil located behind this breaker. This residual current has no direct relation to the faulted phase currents and therefore is phase displaced. This angular displacement can cause some problems for directionality and distance protection measurements[1].

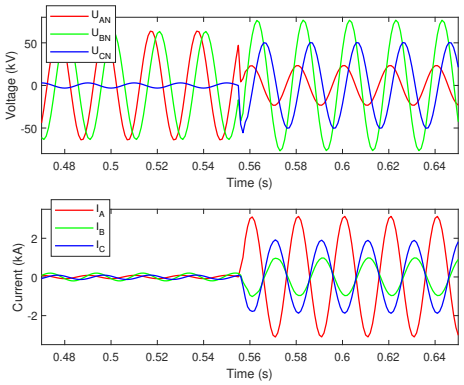

Fig. 11. Voltages and currents at BRK4 for Type IV pattern for simulated fault between F1 and F3.

In order to compensate for the difference between the two faulted current magnitudes and the lack of path through the neutral of the transformer, an artificial increase of the current in the non-faulted Ph-C occurs. This current flows from the side that sees both faults forward (source(s) at BRK4's side) and returns through the source that is located between the faults (source(s) at BRK3's side) [1].

From the perspective of BRK3, located between the two faults, the residual current behavior is completely the opposite. Real recordings from a CCF in a Swedish 77 kV network with resonant grounding were used to validate the results for this position. In this case, the simulated and real system do not have the same voltage level but focus should be put mainly on the patterns. Figure 12 shows the simulated and real-recording voltage signals, where the typical behavior is that of one phase voltage is being very reduced (Ph-C as a close-in fault) while the other is further away and therefore the voltage builds up (Ph-A).

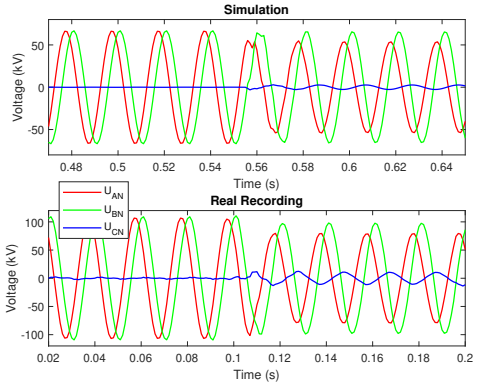

Fig. 12. Comparison of voltages between simulation (in BRK3) and real recording for line with double infeed (Type III) [1].

The currents are also compared in Fig. 13. Since the measurement point, located between the two faults, sees F3 forward and F1 in reverse direction, the currents in phases A and B end up being in phase with each other (almost $0°$). Additionally, Ph-C current which compensates the lack of zero-sequence current flowing from BRK4 side also ends up being in phase with the other two phase currents.

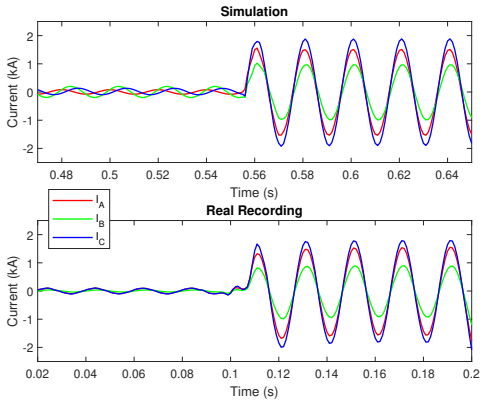

Fig. 13. Comparison of currents between simulation (in BRK3) and real recording for line with double infeed (Type III) [1].

Figure 14 shows the residual current in each side of the line with double infeed. The high residual current originated from the sum of the three currents in phase can be observed for BRK3. On the other hand, the side that observes the two faults forward only has a small residual current originated from the Petersen coils located behind it.

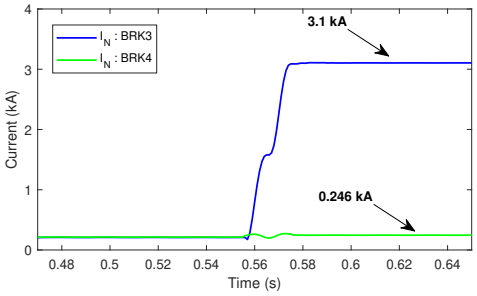

Fig. 14. Simulated remote end of fault measured at BRK4.

Furthermore, the fault location also influences the behavior of the fault currents and the rise of the current in the non-faulted phase for the line end that observes both faults forward, as it is the case for BRK4. Figure 15 shows the same faults as observed in the previous section between F1 (Phase C at a distance of 10% of A_{bus}) and F3 (Phase A distance 90% of BRK4). In this case, since the faults are relatively close to each other, the two faulted phase currents at BRK4 have a quite similar magnitude and are shifted by $180°$, while the effect on the non-faulted phase B is considerably reduced when compared to Fig. 11.

This effect can be further seen in Fig. 16 for measurements at BRK4, where the distance between faults is increased. The current magnitude in F1 (I_C) starts to decrease and the current magnitude in the non-faulted phase (I_B) starts to increase to compensate for the difference between the two-faulted phases and the lack of residual current through BRK4.

In this case, a limit is reached by the two currents where I_B stops increasing and I_C stops decreasing. As faults get further apart from both sources, the contribution to both faults from each source becomes quite similar and therefore the values stabilize. For fault locations in other networks, when sources

are more distant from each other (more than one line apart), these curves can go even lower.

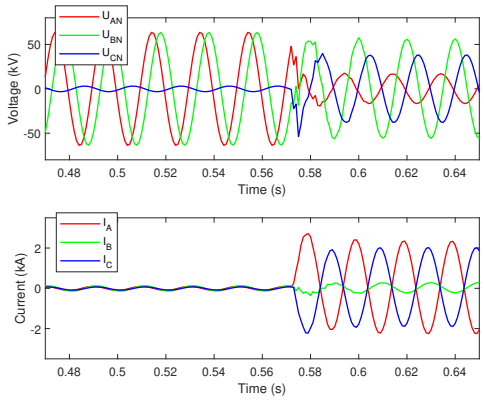

Fig. 15. Simulated remote end of fault measured at BRK4.

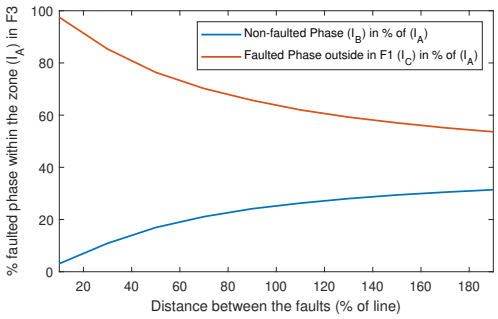

Fig. 16. Effect of distance between faults on currents measured at BRK4.

IV. Conclusions

Different current and voltage patterns presented by Cross-Country Faults in Resonant-Grounded networks have been investigated. Such faults are more complex than common faults seen in the power system. The mathematical model showed important features for such faults, and the simulation models were validated using real faults captured in Scandinavia.

For feeders with single infeed, two different Types I (radial) and II (ring) were defined. Relays measuring Type I CCFs observe a very similar behavior comparing to single phase-to-ground faults in solidly grounded networks, which can make it easy for protection functions to identify such type. Type II, with connection in ring, is influenced directly by the presence of a second phase current, which causes the residual current to decrease and can cause possible problems for protection functions. The fault location in the neighboring feeder has a considerable effect when the fault is closer to the remote end of the feeder.

The fault analysis becomes more challenging when a line has double infeed, where two more Types III and IV were defined. Depending on the position of the measuring relay, the measured residual current can either be considerably higher than any of the faulted phase currents (Type III where the three currents are in phase) or be considerably smaller (Type IV when both faults are seen in forward direction). For Type III, the increase of the current in the non-faulted phase can also have a direct impact on protection relays affecting selectivity, whereas for Type IV the lack of residual current can cause protection functions to not operate for such faults.

For future studies and evaluation of these faults, the transient behavior can be of great interest for analysis and its effects in protection algorithms that need rapid and selective response such as differential and distance protection. Moreover, the effect of phase shift and anomalies in the residual current magnitudes also need to be addressed thoroughly when it comes to phase-to-ground impedance measurements and directional calculation.

References

[1] G. M. G. Guerreiro, "Cross-Country Faults in Resonant-Earthed Networks," M.Sc. Thesis, KTH Royal Institute of Technology, Stockholm, Sweden, October 2020. [Online]. Available: https://kth.diva-portal.org/

[2] C. Figueiredo, G. Mello, and M. Silveira, "Resonant grounding applied in Brazil," *CIRED - Open Access Proceedings Journal*, vol. 2017, no. 1, pp. 1429–1433, 2017.

[3] A. Guldbrand, "Earth faults in extensive cable networks," in *Licentiate Thesis - Lund University - University Department of Measurement Technology and Industrial Electrical Engineering*, 2009.

[4] G. Ziegler, "Numerical distance protection," 4th edition, 2011, [Online ebook version]. Available: www.publicis.de/books.

[5] *Modures: protections de distance statiques types LZ 91, LZ 92, LZ 92-1 : instructions de montage et de service*. Brown, Boveri & Cie BBC, 1985.

[6] A. Codino, F. M. Gatta, A. Geri, S. Lauria, M. Maccioni, and R. Calone, "Detection of cross-country faults in medium voltage distribution ring lines," in *2017 AEIT International Annual Conference*, Sep. 2017, pp. 1–6.

[7] Hitachi ABB Power Grids - Grid Automation Products, "Line distance protection REL670 version 2.2 ANSI - technical manual ABB," 2020. [Online]. Available: www.hitachiabb-powergrids.com/offering/product-and-system/substation-automation--protection---control

[8] P. M. Anderson, *Simultaneous Faults*. IEEE, 1995, pp. 308–344. [Online]. Available: https://ieeexplore.ieee.org/document/5266254

[9] D. Tziouvaras, "Analysis of complex power system faults and operating conditions," *63rd Annual Georgia Tech Protective Relaying Conference, Schweitzer Engineering Laboratories, Inc*, April 2009.